Journal of Power Technologies 100 (2) (2020) 152–160

The influence of surface roughness on the hydrodynamics of the falling water film in cooling towers

Igor Kuzmenko, *Alexandre Gourjii

Abstract

This paper sets out the results of experiments for falling film at $Re_w = 70 \ldots 340$ in the vertical channel of two coaxial tubes, ∅ 37/17 mm, 1 m high, for a countercurrent air flow with $Re_{air} = 2200 \ldots 10^4$. Subject to investigation was falling film on smooth and capillary-porous wall surfaces at constant film thickness greater than the height of the capillary-porous coating (0.3 mm). It was established that film thickness is weakly dependent on the velocity of the countercurrent airflow at $w_{air} = 1.7 \ldots 7.3$ m/s. The water concentration on a smooth surface is 2 times higher at the same film thickness. The results of flooding in a channel with a smooth wall surface confirm the validity of the Wallis equation with deviation up to 20%.

Keywords: falling film, countercurrent flow, capillary-porous wall surface, film thickness

1 Introduction

Study of the features of physical processes in cooling towers, such as contact heat exchangers, is an important scientific and engineering area in energy research. Many researchers focus on two-phase gas-liquid flows, as changing parameters of the liquid phase on solid surfaces can lead to a significant change in thermal characteristics [1]. Therefore, control and management of the parameters of two-phase flows are of great practical importance in atmospheric cooling towers.

A cooling tower contains regular surfaces, which consist in part of vertical channels. Here, the gas flow moves in the opposite direction to the gravitational runoff of the liquid phase, forming a thin falling film on a solid surface. The interaction in atmospheric cooling towers of a liquid film with a gas flow can lead to the onset of the flooding in the devices. This mode ultimately limits the steady and controlled operation of such devices [2].

Modern scientific literature pays special attention to the study of liquid film dynamics in a gas flow. Here we need to highlight the classic work of Nusselt [3] in which the dependence of the thickness of a liquid film during gravitational flow along a vertical flat surface is given. Many researchers [4] have experimentally studied the interaction of a gas flow with a liquid film. For example, Hewitt and Wallis [5] considered the features of liquid film flow in the range of Reynolds numbers values for the wave motion of the film $Re_w < 10^3$ without the presence of a gas flow. An empirical dependence of the thickness of the liquid film δ on its rate of flow was established in the work, which in the above-mentioned Re_w (see eq. 2 below) range was about 1.6 times higher than the Nusselt data for a smooth film.

Dyakowski and Stefański studied [6] water film flowing at the plate 0.5x3 m with inclination angle 0-90°. They suggested using autocorrelation coefficient to evaluate the regime of wave motion of a water film at $Re_w = 220$ and 500.

Zadrazil and Markides [7] researched the recirculation zones within water waves. Experiments were used for optical diagnostic techniques in the downwards annular flow at Re ranges for the water/air phases of Re_w 306...1532 and Re_{air} 0...84600, respectively.

The authors found that the local mean film thickness was within 10% for the falling films and 20% for recirculation zones within a wave.

Wan et al. described [8] the techniques for measuring the thickness of a falling film in a two-phase horizontal annular flow, empirical correlations for film thickness in microchannels and suchlike.

Ito et al. [9] measured local thickness of water films of the air–water upwards flow in narrow channel. The authors studied the bubbly flow, slug flow and churn flow that passed through the test section at a height of 900 mm from the air inlet. The film thickness varies from 50 to 550 μm per 0.2 second in the case of churn flow.

Feind [10] showed that the turbulent flow in a liquid film on a smooth vertical surface develops at $Re_w > 1200$. The author established the empirical dependence of the liquid film thickness without the pres-

*Igor Sikorsky Kyiv Polytechnic Institute, Kyiv, Ukraine, ozirno@gmail.com

ence of the gas flow on Reynolds numbers Re_w. It was shown that the values δ are proportional in the first approximation to $Re_w{}^{0.5}$.

The empirical dependence of the thickness of the water film on a rough surface (with knurling) without gas flow on Reynolds numbers in the diapason $15 < Re_w < 16800$ in a tube with a height of 591 mm was shown in the book [1]. It was established that the values of the film thickness over the surface with roughness $\delta*$ is determined by the sum $\delta* = \Delta + \delta$, where δ is the film thickness, Δ is the average roughness size.

Detailed analysis of the physical processes in the vertical channels of cooling towers shows that the onset of the flooding regime is accompanied by a sharp change in various hydrodynamic parameters. This gave various methods for identifying the flooding regime. On the one hand, it was shown [2], [11], [12] that the flooding process is characterized by a sharp increase in the pressure gradient, caused by an increase in the amplitude of waves on the film surface. On the other hand, Pushkina et al. [13] define the onset of flooding mode as the sharp development of capillary waves on the interface surface of a film with an airflow. It was established experimentally that the value of Kutateladze number $K_w \approx 3.2$ (see eq. 6 below) in a wide range of diameters (20 ... 203 mm) and lengths (1.75 ... 3.40 m) of the channel.

Zhao et al. [14] described the waves in water film at upward annular air-water flow. It was established experimentally that wave frequency decreases and amplitude increases with growing film thickness at $Re_w = 211 \ldots 603$.

Wallis [15] notes that the onset of the flooding regime is determined by using semi-empirical correlation between dimensionless velocity of gas and fluid in the cross section of the channels.

Cioncolini and Thome [16] on the basis of semi-empirical correlation presented nine empirical equations for predicting the entrained liquid fraction with a large experimental database of authors for two-phase flow in an annular regime.

Hussein et al. [17] created a CFD model of the churn flow in a 3-inch diameter vertical tube for different liquid flow rates. Simulations were carried out using the commercial software ANSYS Fluent in the upward vertical flow regime of air and water. The model showed oscillatory behaviors of shear stress and pressure, but the calculated results of water film thickness were not compared to experimental results.

Analysis of modern scientific literature shows that little research effort has been directed toward the problem of the effect of a capillary-porous surface completely flooded with liquid on the interaction parameters of a liquid film with a gas flow in vertical channels of cooling towers. The effect of the type of surface of the channels and the velocity of countercurrent gas flow on film thickness in vertical channels remains unclear. The dependence of the pressure gradient values in the gas flow on film thickness on different surfaces of channel is of practical interest. The main goal of this work is to determine the hydrodynamic parameters of the onset of the flooding mode in the system of vertical coaxial channels with a completely submerged (hydraulically smooth) capillary-porous surface.

This article is organized as follows: The first section provides a brief description of the experimental setup, measuring equipment, and a brief analysis of accuracy values of measuring physical quantities. The second section analyzes the experimental dependences obtained for two types of surfaces (smooth and capillary-porous surfaces) in the channel made from two coaxial tubes. The last section gives general conclusions.

2 Experimental setup

Laboratory studies were carried out in the Heat power engineer department of the National Technical University of Ukraine: Igor Sikorsky Kyiv Polytechnic Institute. The experimental stand is shown schematically in Fig. 1.

The main element of the stand is the working section (I) in the form of a vertical coaxial channel. The Roman numeral II denotes the air supply line, which consists of the ELPROM-LOVE4-380W blower (1), the adjusting valve (2), glass rotameter RS-7 (3) with several ranges of gas flow measurement scales and the electric heater (4). The water supply line (III) consists of an adjusting valve (5), a glass rotameter RS-3 (6) and an electric heater (7).

The overflow water irrigator (8) is placed at the input of the working section. It forms a uniform thin film on the outer surface of the inner tube (9). The inner surface of the outer tube (10) in the experiment remains dry. The liquid collector (11), which collects and removes liquid from the surface of the inner tube, is placed in the lower part of the working section. There is also a MMN-240 manometer (12) with an inclined tube for measuring overpressure in the lower part of the working section. The design of the working section (I) of the experimental setup is shown in Fig. 2.

The working section consists of two coaxial tubes with a height of $H \approx 1$ m; the total length of the tubes is about 1.16 m, including tube sections allocated to the water irrigator (8) above and a liquid collector (11)

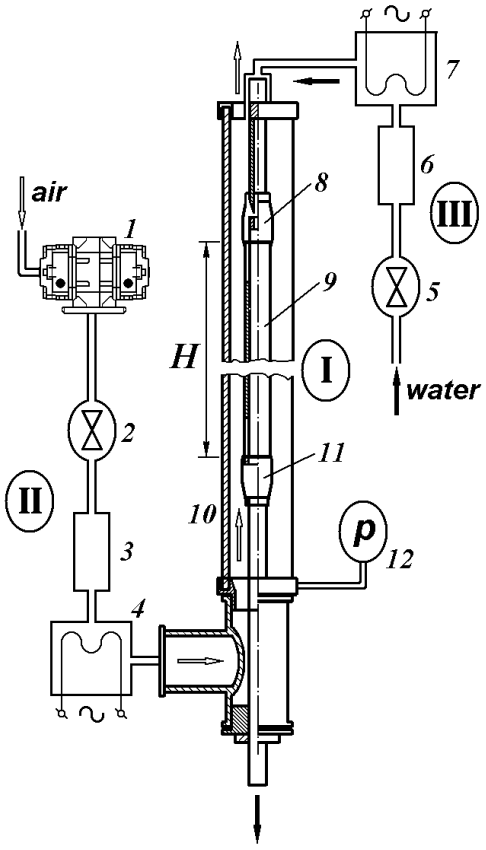

Figure 1: Schematic diagram of the experimental stand with a working section (I), air (II) and water (III) supply lines

below. The inner tube was made of stainless steel X18H10T with an outer diameter $d = 16.0$ mm. The outer surface of the inner tube is machined with an average roughness about of 5 10^{-5} m.

The outer tube of the working section is a glass tube with an inner diameter $D = 37.0$ mm. The inner tube of stainless steel was laid down in water before assembling the working section for 50-100 hours to increase adhesion force and uniform distribution of the liquid film on the surface of the inner tube.

After complete installation of the entire working section, the vertical position of the working section of the stand was checked.

The second part of the experiments were carried out with the working surface of the inner tube covered with a mesh (13) (Fig. 3). The mesh was a system of square cells with dimensions of 0.56 × 0.56 mm, which served as a capillary-porous coating made of wire with a diameter of 2.5 10^{-4} m.

The width of the mesh surface was chosen so that

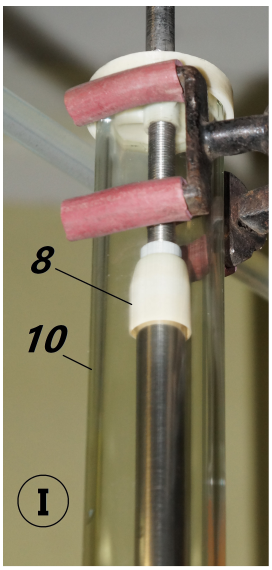

Figure 2: Photo of the working section of the experimental stand

the edges of the mesh lay close to the weld. Before the experiments, the working section with the welded mesh surface was degreased. In this case, the outer diameter of the tube increased and was equal to $d \approx 17$ mm. During the experiments, the structure of the capillary-porous surface was completely covered with a water film, as shown schematically in Fig. 3.

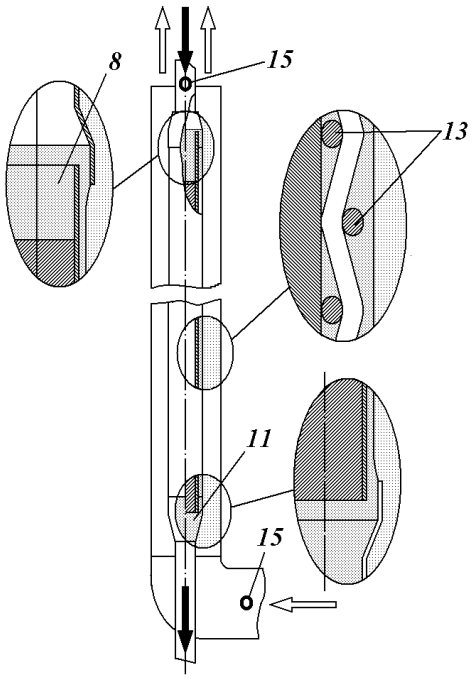

Figure 3: Schematic diagram of the working section with a capillary-porous coating

The temperatures of air T_{air} and water T_w, volumetric flow rates of air Q_{air} and water Q_w, film volume J on the outer surface of the inner tube, overpressure ΔP in the lower part of the working section were controlled in the experiment. The temperature of the water film and air was measured with an accuracy of 0.05 °C with a chromel-alumel Cr/Al thermocouple converter connected to the recording device UKT38-Sh4.AT. Volumetric flow rate of air was measured by a rotameter (3) with the calibrated accuracy of 2.8 10^{-5} m^3/s, and volumetric flow rate of water was controlled by a rotameter (6) with an accuracy of 4.2 10^{-8} m^3/s.

The volume of the held up water film J on the outer surface of the inner tube was determined by the cut-off method. This method consists of interrupting the supply of water and air upon reaching a stationary interaction regime and the subsequent measurement of the water volume collected from the surface of the inner tube in the working section. Measurements of the volume of collected water were carried out with an accuracy of 5.0 10^{-7} m^3. The overpressure was measured by a manometer (12) connected through a pulse tube with a diameter of 0.8 mm with a drip-catcher, which prevents liquid from entering the device. The accuracy of the pressure measurement reached 0.1 Pa.

The tap water supplied after the electric heater (7) is uniformly distributed around the outer surface of the inner tube by the overflow water irrigator (8) (fig.3). Water from the top of the irrigator fills the selected volume up to the edge of the irrigator, combined with the surface of the inner tube. Further flow of water leads to a liquid overflow and the formation of a uniform liquid film on the outer surface of the inner tube.

After that a water film falling along the outer surface of the inner tube enters a specially designed collector (11) (Fig. 3), which practically does not disturb the air flow directed upwards. Then the water film is discharged into the drainage through the hydraulic lock. An inner tube with the overflow water irrigator (8) and collector with hydraulic lock are mounted inside an outer glass tube. The airflow after the heater, temperature-controlled by a thermocouple, goes into the working section. To determine the temperature at the control points, chromel-alumel Cr/Al thermocouples (15) with a junction of a thermocouple ∅ 0.5 mm were used. Thermocouples placed inside the airflow have mesh screens that prevent liquid from entering the device. Water temperature was measured at the inlet and outlet of the working section, in front of the water irrigator and in the collection.

The first series of experiments was carried out for the gravitational falling water film without an airflow. The thickness of the gravitational water film was determined by the equation

$$h = \frac{J}{\pi d H} \tag{1}$$

The accuracy of the calculated h was about 2.5%

The regime of the falling water film was determined by the Reynolds number

$$Re_w = \frac{4Q_w}{\nu_w \pi d} \tag{2}$$

where: ν_w - the kinematic viscosity of water.

The accuracy of the calculated Re_w was approximately 4.6%.

A second series of experiments was carried out to establish the distinctive features of a falling water film along the smooth and capillary-porous outer surfaces of the inner tube at constant volumetric flow rates of countercurrent air ($Q_{air} = const$). The characteristic parameters of airflow in this case are the velocity of air

$$w = \frac{4Q_{air}}{\pi(D^2 - d^2)} \tag{3}$$

and the Reynolds number

$$Re_{air} = \frac{w(D-d)}{\nu_{air}} \tag{4}$$

where: ν_{air} - the kinematic viscosity of air.

The accuracies of the calculated w and Re_{air} were approximately 4.3% for each one.

The third series of experiments is devoted to defining features of a falling water film along smooth and capillary-porous surfaces at constant film thickness ($Q_w = const$, $h = const$). The main parameter in this case was the volumetric flow rates of air Q_{air}, which is determined by the pressure gradient $\Delta p/\Delta z$ within the channel of two coaxial tubes.

The ranges of parameter changes of the gravitational water film and the countercurrent air flow in the above-mentioned experiments are presented in Table 1. Three series of experiments were carried out independently for the smooth and capillary-porous outer surfaces on the inner tube.

Tabelle 1: The ranges of measurement parameters in the experiments

N	Section	Channel with mesh	Smooth channel
1	Temperature of film, °C	10(20)	10
2	Temperature of air, °C	18	12
3	Re_w	1.7 10^2...3.0 10^2	1.4 10^2 ...3.4 10^2
4	Re_{air}	2.5 10^3...6.2 10^3	2.9 10^3 ...1.0 10^4
5	w_{air}, m/s	1.8...4.5	1.8...7.3
6	Γ, kg/(m sec)	0.042...0.085	0.08...0.12
7	h, m	0.19 10^{-3}...0.42 10^{-3}	0.35 10^{-3}...0.49 10^{-3}

When processing N series of experimental values (x_i and y_i), the value of the correlation coefficient between the data was determined by following [18]

$$R = \frac{\sum_{i=1}^{n}(x_i - \overline{x})(y_i - \overline{y})}{\sqrt{\sum_{i=1}^{n}(x_i - \overline{x})^2 \sum_{i=1}^{n}(y_i - \overline{y})^2}} \qquad (5)$$

where

$$\overline{x} = \frac{1}{n}\sum_{i=1}^{n} x_i$$

$$\overline{y} = \frac{1}{n}\sum_{i=1}^{n} y_i$$

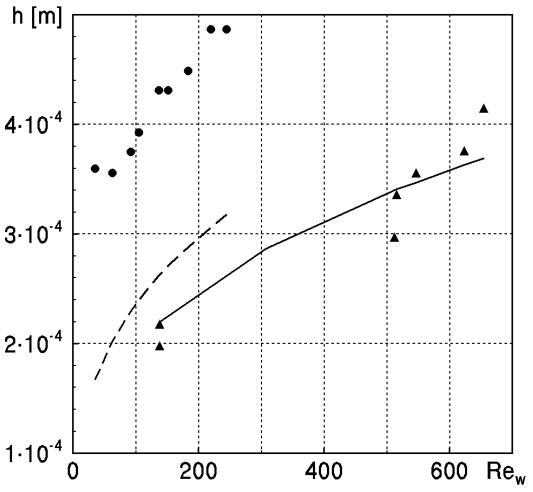

Figure 4: Dependence of the thickness of the gravitational flowing film on the number of Re_w in the coaxial channel with various types of surfaces

3 Experimental Results and Discussion

The first series of experiments is devoted to the study of the dependence of film thickness on the velocity of falling film along the outer surface of the inner tube. The triangles in Fig. 4 show the experimental data for the case of a smooth surface ($T_w = 20$ ℃) and the circles show similar results for a capillary-porous surface ($T_w = 10$ ℃). It is seen that an increase in film thickness leads to an increase in the values of gravitational fluid flow.

The solid lines in the figure show the calculation results for the analytical dependencies presented in [3] for a smooth surface. The experimental data and analytical calculations practically coincide with a deviation of up to 15% in the range of Reynolds numbers $Re_w = 150 \ldots 650$ for a smooth surface. For the case of a capillary-porous coating, the experimental data (circles) exceeds the analytical calculations (dashed line) by 30-50% in the range $Re_w = 20 \ldots 350$. These differences are explained, as the volume of held up fluid J on the capillary-porous surface was more than on the smooth outer surface of the inner tube.

Use of a countercurrent airflow in the experiment increases the volume of held up fluid J on the outer surface of the inner tube. Fig. 5 shows the dependence of film thickness on water concentration

$$\Gamma = \frac{Q_w \rho}{\pi d}$$

The triangles show experimental data for a smooth tube with countercurrent airflow ($Re_{air} = 5800$, $w = 4.6$ m/s), and the solid line shows the results of numerical calculations [3] performed for a smooth outer surface of the inner tube without airflow. In this case the local increase in film thickness by 10...40% is caused by the influence of viscous shear forces on the interface between media moving in the opposite directions.

In the experiment with a capillary-porous surface, the value of the film thickness increases compared with

the case of a smooth surface for the same values of water concentration (Fig. 5). The figure shows experimental film thickness for the case $w = 1.8$ m/s (Re_{air} = 2300) with circles, while diamonds denote data for $w = 3.1$ m/s (Re_{air} = 3950) and squares show data for air velocity $w = 4.5$ m/s (Re_{air} = 5800). Experimental data on the dependence of film thickness in a coaxial channel with a capillary-porous surface on the water concentration correspond to large values of the correlation coefficient $R = 0.9$. They are generalized by a single curve, which is plotted with a dashed line in Fig. 5 in the range of velocities of air flow $w = 1.8 \ldots 4.5$ m/s. Note that in all experiments film thickness exceeded the thickness of the capillary-porous coating.

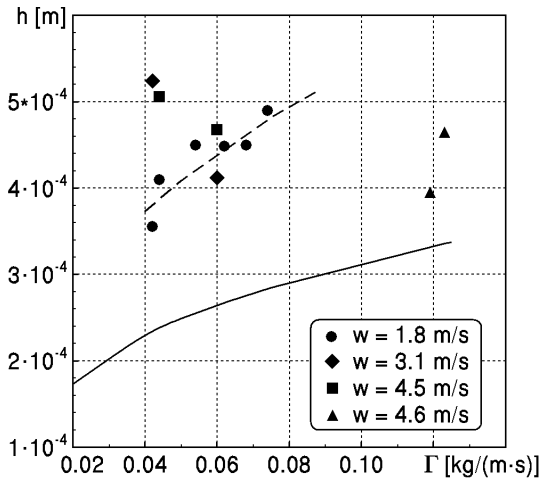

Figure 5: Dependence of the thickness of the gravitational flowing film on water concentration for the outer surface of the inner tube with various types of surfaces

Data analysis show that the use of a capillary-porous coating of outer surface of inner tubes in channels can be used to increase the falling film thickness by 1.5 ... 3.0 times in the range of velocities of countercurrent airflow $w = 1.8 \ldots 4.5$ m/s. It should be noted that the capillary-porous coating reduces the water concentration values Γ by about 2 times compared to the case of a smooth surface at the same values of film thickness.

Fig. 6 shows the dependence of the pressure gradient $\Delta p/\Delta z$ within the channel of two coaxial tubes on the density of irrigation Γ with an oppositely directed airflow for different values of air velocity w. The figure is plotted with notation similar to fig. 5. It is seen that for small values of airflow velocity, an increase in water concentration Γ leads to a gradual decrease in the values of pressure gradient upon reaching the stationary regime. When $w = 4.5$ m/s (Re_{air} = 5800), this tendency disappears and the pressure gradient does not actually depend on the values of the water concentration on the capillary-porous surface. Thus the value of the pressure gradient $\Delta p/\Delta z$ remains the same when significantly increasing the values of water concentration Γ for velocity of airflow $w = 4.5 \ldots 4.6$ m/s in a channel with a capillary-porous coating on the outer surface of the inner tube.

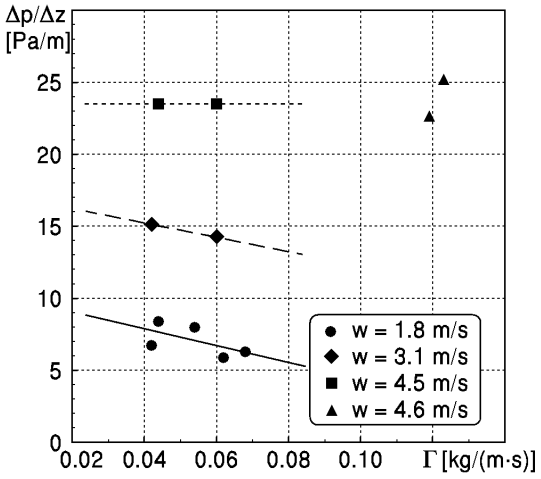

Figure 6: Dependence of the pressure gradient $\Delta p/\Delta z$ in the channel on the water concentration Γ with different types of surfaces

An analysis of the data presented in Fig. 6 shows that the velocity-pressure relationship differs from the quadratic dependence. This effect is explained by the presence of a moving interface between liquid and gaseous media. For example, increasing the velocity of airflow from 1.8 m/s to 3.1 m/s (1.7 times) causes an increase in the values of the pressure gradient $\Delta p/\Delta z$ from 5.8 Pa/m to 14.3 Pa/m (2.5 times) in the working section of the experimental stand.

A third series of experiments was devoted to the study of the dependence of the hydrodynamic parameters of the water film on the velocity of airflow at constant volumetric flow rates of water Q_w.

Fig. 7 illustrates the relation between the thickness of the falling water film and the velocity of air motion ($w = 1.8 \ldots 7.3$ m/s, Re_{air} = 2450 ... 10100) in the channel of two coaxial tubes. The experimental data at the smooth outer surface of inner tube in this figure are shown by triangles that approximated to a solid curve by the least-squares method [18]. The experiments were carried out with water concentration values in the range of $\Gamma = (6.0 \ldots 8.0)\ 10^{-2}$(kg/(m s).

It can be seen that the thickness h of the water film does not depend on the velocity w of the airflow in the first approximation. This conclusion is confirmed by the low value of the correlation coefficient R ≈ 0.2.

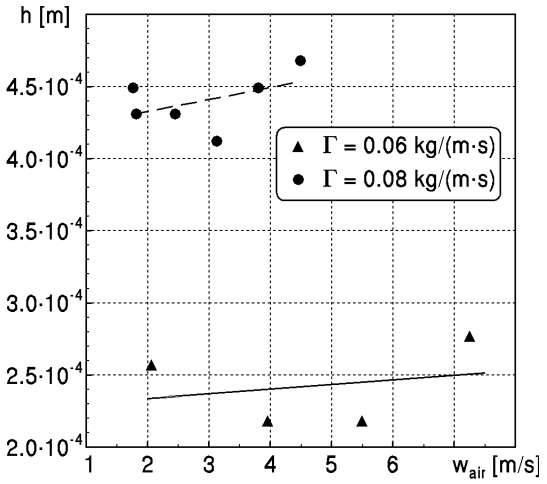

Figure 7: Dependence of the thickness of the gravitational flowing film on the number of Re_w in the channel with different types of surfaces

In Fig. 7 circles show similar experimental data obtained on a capillary-porous surface, and the approximation curve is plotted as a dashed line. This part of the experiment was carried out at a constant water concentration value. We can see that the thickness of the falling water film has a weak dependence on the velocity of airflow in the specified range of values of water concentration Γ on the outer surface of the inner tube as the correlation coefficient reaches value R ≈ 0.5.

A comparative analysis of the data presented in Fig. 5 and Fig. 7 shows that film thickness h on a capillary-porous surface is 1.7...2.0 times greater than film thickness h on a smooth surface over the entire studied velocity range w of countercurrent airflow at equal values of water concentration Γ.

The dependence of the pressure gradient $\Delta p/\Delta z$ in the channel on airflow velocity w is shown in Fig. 8. The triangles, as before, show experimental data for the smooth surface with water concentration Γ = 0,085 kg/(m s) (Re_{air} = 2900...10100), the data obtained for capillary-porous surface in the range of water concentration Γ = 0.042...0.062 kg/(m s) (Re_{air} = 2500...6200) are shown by the circles. The approximation line "pressure gradient-air velocity" was shown on the figure for different types of surfaces. Therefore, the surface of the liquid

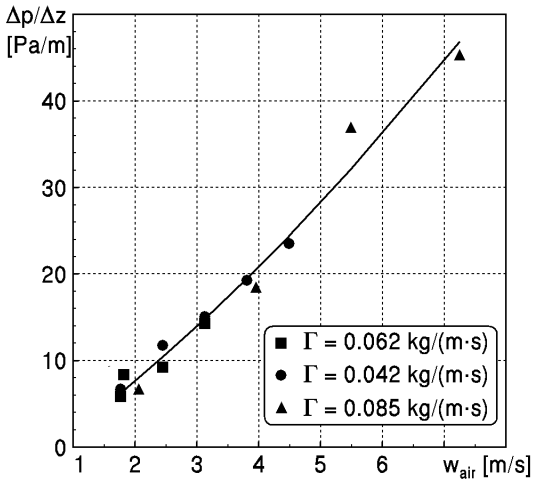

Figure 8: Dependence of the pressure gradient $\Delta p/\Delta z$ on air velocity w in the channel

film above the capillary-porous coating was a smooth and unperturbed one. The experimental data are summarized by a curve with a deviation of up to 15%.

An analysis of the data presented in Fig. 8 shows that a change in airflow velocity in the range of values w = 2.0...4.0 m/s corresponds to a change in pressure gradient in the range of values $\Delta p/\Delta z$ = 7.7...20.5 Pa/m. So, the dependency of the pressure gradient on the velocity of the airflow differs from the quadratic one to a smaller degree and does not depend on the type of outer surface of the inner tube.

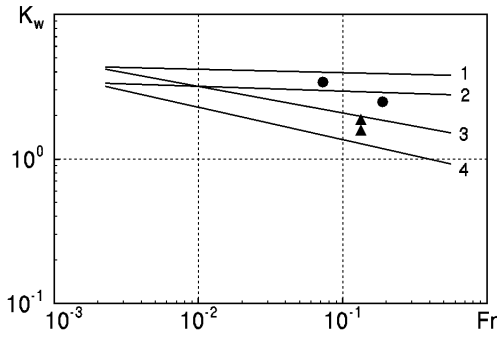

Figure 9: Dependence of the values of the Kutateladze number K_w on the Froude number Fr in the experiment for values Bo = 20: 1 – Wallis (c=1.0), 2 – Wallis (c=0.88) [15], 3 – Pushkina [13], 4 – Tobilevich [2]

An important similarity criterion of the hydrodynamic interaction of a gas flow with a liquid film are

Kutateladze number K_w and Froude number Fr and Bond number Bo for a vertical channel. A classic definition of similarity numbers can be found in [2]. In our case

$$K_w = \frac{w_{air}\rho_w^{0.5}}{(\sigma g(\rho_w - \rho_{air}))^{0.25}} \quad (6)$$

$$Fr = \frac{Q_w}{(g\delta^3)^{0.5}}$$

$$Bo = \frac{d}{\delta}$$

where $\delta = \sqrt{\sigma/g(\rho_w - \rho_{air})}$ is the Laplace constant, w_{air} – the average velocity of airflow in the cross section of the tube, ρ_w and ρ_{air} – the water and air densities, g – gravity acceleration, σ – surface tension coefficient of water, d – diameter of the channel.

The accuracies of the calculated K_w and Fr were about 4.7% and 3.9% respectively.

The accuracies of the calculated Bo and d were about 1.8% for each one.

Wallis [15] established the dependence of the beginning of the flooding process on the parameter

$$c = \sqrt{W_w^*} + \sqrt{W_{air}^*}$$

where W^*_w and W^*_{air} are the normalized values of the average velocities of the liquid and gas in the channel. It is shown that the critical value of the parameter is in the range of $c = 0.88 \ldots 1.00$.

Fig. 9 shows the dependencies of the value K_w on the Froude numbers Fr, presented by various authors for Bond number $Bo = 20$. The data of our experiment for the smooth outer surface of the inner tube ($\Gamma = 0.033 \ldots 0.085$ kg/(m s), $w = 7.2 \ldots 10$ m/s, $Re_w = 130 \ldots 330$, $Re_{air} = 10000 \ldots 13900$) are shown by circles, while triangles indicate data for a case with a capillary-porous surface ($\Gamma = 0.059 \ldots 0.060$ kg/(m s), $w = 4.6 \ldots 5.5$ m/s, $Re_w = 235 \ldots 240$, $Re_{air} = 6400 \ldots 7600$). It can be seen that the experimental data on a smooth surface correspond to the experimental data of Wallis [15] in the presence of a flooding process (with coefficient c = 0.88) with accuracy of ±20%. Curve 3 in Fig. 9 is plotted in Pushkina's results [13] for a wide range of diameter values (20…203 mm) and lengths (1.75…3.4 m) of channels. The experimental data of Tobilevich [2] (line 4) were obtained for a two-phase water/water steam system in channels of 2.5…3.0 m in height and 33…53 mm in diameter.

In the experiment, it was visually observed that with an increase in gas flow velocity, there was a violation of the stability of the falling water film. This led to the onset of flooding. The triangles and circles in fig. 9 correspond to the destruction of the water film, as calculated by values of K_w.

Analysis of the data shows that the flooding phenomenon in the channel with a smooth surface takes place at a greater velocity of airflow compared with the capillary-porous surface. The number K_w for the smooth surface takes values of about 1.2…1.3 times more than for the capillary-porous surface in indicated ranges of water concentration Γ and velocity w of the airflow. This effect is explained by the large value of the film thickness on the capillary-porous surface compared to the smooth surface at the same hydrodynamic parameters of the water and gas flows (see Fig. 5).

4 Conclusions

Experimental studies of hydrodynamics in cooling towers are devoted to identifying the general laws of the hydrodynamic parameters of the gravitational film motion with countercurrent airflow.

It is shown that film thickness in the vertical channel with a capillary-porous coating is 30-50% larger than film thickness with a smooth channel at the same values of water concentration ($\Gamma = 0.04 \ldots 0.12$ kg/(m s)) and gas flow ($Re_{air} = 2300 \ldots 5800$). The main reason for increases in the thickness of the falling film is the greater value of local resistance to the fluid film motion compared to the case with a capillary-porous surface.

It was experimentally confirmed that the film thickness in the first approximation is proportional to the water concentration of the outer surface of the inner tube. A comparison of the dependences obtained shows that the use of a capillary-porous surface can be used to increase film thickness by approximately 1.5-2.8 times compared to a smooth surface at the same water concentration Γ in the range of $\Gamma = 0.04 \ldots 0.08$ kg/(m s). The use of a capillary-porous surface makes it possible to achieve the same values of film thicknesses with smaller values (approximately 2 times) of water concentration Γ compared to a smooth surface.

It is shown that the dependence of the pressure gradient on the water concentration for large values of the gas velocity disappears and becomes a constant value. This effect takes place for various types of surfaces. The thickness of the liquid film actually shows a weak linear dependence on the velocity of airflow. However, the amplitude value of the film thickness for a capillary-porous surface is about

1.7. . . 2.0 times larger than for a smooth surface at the same velocity of airflow.

It was established experimentally that the onset of the flooding regime in a channel for the laminar regime of the falling film along the capillary-porous surface compared to the falling film along the smooth surface is 20-30% lower under conditions of a countercurrent airflow.

References

1.Vorontsov Ye.G., T.Y.U.M. (1972) *Teploobmen v zhidkostnykh plenkakh*, Kyiv: Tekhnika.

2.Bezrodny M.K., K.N.O., Pioro I.L. (2005) *Transfer processes in two-phase thermosyphon systems. Theory and Practice*, Fact.

3.W., N. (1916) De oberflachenkondensation des waserdampfes. *Z. VDI*, **60**.

4.Bankoff, S., and Lee, S. (1983) Critical review of the flooding literature.

5.Hewitt G.F., W.G.B. (1963) Flooding and associated phenomena in falling film flowing a vertical tube. *UKAEA Report*, **AERE-R4022**.

6.T. Dyakowski, J.S. (1981) The qualification of the kind of wavy motion of liquid layer by analysis of changes of its thickness in time. *29-39, Information bulletin of the institute of Heat Technology Warsaw University of Technology*, **58**.

7.Zadrazil, I., and Markides, C.N. (2014) An experimental characterization of liquid films in downwards co-current gas–liquid annular flow by particle image and tracking velocimetry. *International Journal of Multiphase Flow*, **67**, 42–53.

8. (2020) A technical review of research progress on thin liquid film thickness measurement. *Experimental and Computational Multiphase Flow*, **2, N4**.

9.Ito, D., Damsohn, M., Prasser, H.-M., and Aritomi, M. (2011) Dynamic film thickness between bubbles and wall in a narrow channel. *Experiments in Fluids*, **51** (3), 821–833.

10.K., F. (1960) Stromungsuntersuchung hei Gegenstrom von Rieselfilm und Gas in lotrechten Rohren. *VDJ-Forschangsheft*, **4-81, 150**.

11.V.O., T. (2010) Teplomasoobmin i hidrodynamika paro hazoridynnykh potokiv v kanalakh z sitchastym pokryttyam.

12.Celata, G.P., Cumo, M., and Setaro, T. (1992) A data set of flooding in circular tubes. *Experimental Thermal and Fluid Science*, **5** (4), 437–447.

13.Pushkina O.L., S.Y.L. (1969) Breakdown of Liquid Film Motion in Vertical Tubes. *Heat Transfer, Sov. Res.*, **1**.

14.Zhao, Y., Markides, C.N., Matar, O.K., and Hewitt, G.F. (2013) Disturbance wave development in two-phase gas–liquid upwards vertical annular flow. *International Journal of Multiphase Flow*, **55**, 111–129.

15.Hogan, K.J. (2009) A mechanistic model for flooding in vertical tubes.

16.Cioncolini, A., and Thome, J.R. (2010) Prediction of the entrained liquid fraction in vertical annular gas–liquid two-phase flow. *International Journal of Multiphase Flow*, **36** (4), 293–302.

17.Hussein, M.M., Al-Sarkhi, A., Badr, H.M., and Habib, M.A. (2019) CFD modeling of liquid film reversal of two-phase flow in vertical pipes. *Journal of Petroleum Exploration and Production Technology*, **9** (4), 3039–3070.

18.Lieblein, J., Korn, G.A., and Korn, T.M. (1961) Mathematical Handbook for Scientists and Engineers. *Mathematics of Computation*, **15** (76), 421.